Indirect transmission and disinfection strategies on heterogeneous networks

Su Zhong, Xiaoqun Wu,* and Yanting Li
School of Mathematics and Statistics, Wuhan University, Wuhan, 430072, China
and Hubei Key Laboratory of Computational Science, Wuhan University, Wuhan, 430072, China

Congying Liu†
School of Mathematics and Statistics, Jiangsu Normal University, Jiangsu 221116, China

(Received 30 January 2022; revised 20 September 2022; accepted 1 November 2022; published 23 November 2022)

Besides direct contacts of individuals, indirect contacts with environments being the medium is another route of epidemic transmission, which most previous studies have ignored. Disinfection is one of the most effective and commonly used measures to prevent and control epidemic spreading. In this paper, we propose a metapopulationlike model incorporating direct and indirect transmissions for susceptible-infected-susceptible-like epidemics on heterogeneous networks. Furthermore, we explore the epidemic spreading process with heterogeneous disinfection on both spatial and time dimensions. Specifically, we put forward three types of disinfection strategies, namely, the static disinfection strategy, the random time disinfection strategy, and the event-triggered disinfection strategy. Comparative analysis of the three strategies suggests that managers should prioritize disinfection resource allocation to large-flow environments, especially when disinfection resources are limited. In addition, timely disinfection of environments with infected visitors is an effective and economical strategy. Our model sheds light on the interplay dynamics of indirect transmission and disinfection and the results provide theoretical support for governors to select proper disinfection strategies in practical scenarios.

DOI: 10.1103/PhysRevE.106.054309

I. INTRODUCTION

Mathematical epidemic models based on complex networks [1–3] play an essential role in understanding the spreading process of epidemics and providing theoretical methods for epidemic prevention and control. For airborne diseases such as COVID-19, the gathering of individuals and their movements among different environments are the main factors causing epidemic spreading. In this scenario, the social contacts of individuals can neither be seemed as completely well-mixed nor networked. Thus, the metapopulation model [4–6] has become an effective tool for studying such an intermediate-level case.

In metapopulation models, each node represents a subpopulation where all individuals are well mixed. Links among nodes depict individuals' movement routes among subpopulations. There have been many works based on the metapopulation model with various assumptions about mobility patterns, epidemic dynamics, and network structures [7–11]. Most of them treated subpopulations as the meeting sites of individuals. However, they did not capture some critical real-world features, such as individuals getting infected by the pathogens in the environment. In fact, besides direct contact with the current infected visitors of an environment, susceptible individuals can also be infected indirectly by contacting water, air, or objects contaminated by previous infected visitors. In this situation, environments are not only meeting sites of individuals but also, in a way, infectious pathogens carriers themselves. Recently, in scenarios where individuals follow the recurrent mobility pattern [10,12], some researchers [13,14] proposed a special metapopulation model that divided the subpopulations into two disjoint parts: residences and locations. Under a proper spatial scale, they successfully showed the impact of environments as meeting sites on epidemic spreading. Moreover, they provided us with a framework to further study the role of environments when they can keep infectious pathogens.

Disinfection is a well-used measure to eliminate pathogens and reduce indirect transmission in the environment. Previous studies [15–17] taking both indirect transmission and disinfection into consideration have only one environment. These models are inapplicable when there are multiple environments following independent disinfection schedules. Moreover, since environments will keep receiving infectious pathogens from their infected visitors, disinfecting environments for one time cannot rid the environment of pathogens forever, which means we have to disinfect each environment at intervals. On this condition, the disinfection strategy of deciding when and how often we disinfect an environment is an urgent issue that needs to be considered. Compared with the immunization strategy and the heterogeneous intervention strategy [18–20] (a spatial resource allocation strategy based on the metapopulation model), the disinfection strategy also needs consideration in the time dimension. We innovatively model the interplay dynamics of indirect transmission and disinfection on heterogeneous networks and further explore disinfection strategies.

In this paper, we use the discrete-Markov method [13,21] to establish a metapopulationlike model with epidemic dynamics being a susceptible-infected-susceptible-like (SIS)

*Corresponding author: xqwu@whu.edu.cn
†Corresponding author: cyliu@jsnu.edu.cn

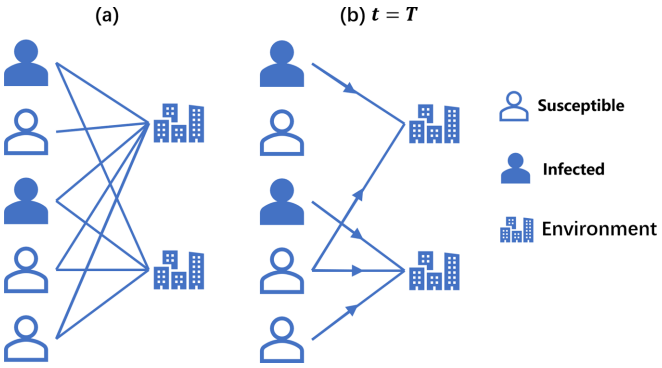

FIG. 1. (a) Model network with five individuals and two environments. (b) Movements of individuals at $t = T$. Arrow lines represent the individuals visiting the environments at $t = T$.

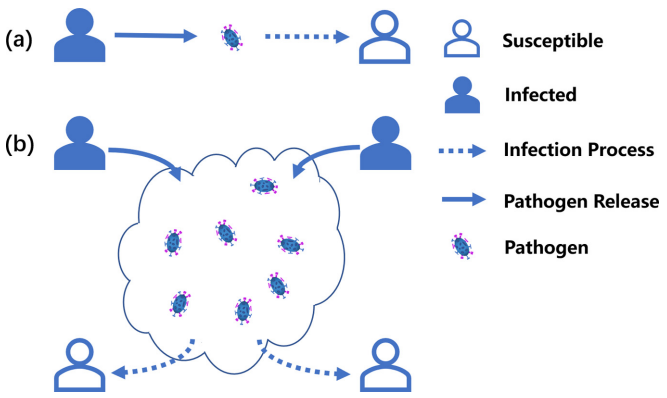

FIG. 2. (a) The infection process between a infected individual and a susceptible individual. (b) The infection process in an environment with two infected individuals and two susceptible individuals.

infection process. We build the model on a bipartite graph with N individual nodes and M environment nodes. Each individual has an independent and uniform chance to visit their neighboring environments at each time step. All visitors of an environment at the same time step are well-mixed. Infected visitors will release pathogens into the environment, and these pathogens can infect other susceptible visitors. Part of pathogens remains infectious to the next time step. We make necessary assumptions on the time evolution of pathogens and the infectivity of environments (see Sec. II A for more details). In our model, disinfection involves the spreading process by preventing pathogens from remaining infectious to the next time step. We find that the disinfection strategy greatly influences the prevalence of epidemics. Specifically, we propose three types of disinfection strategies and compare their effects on suppressing epidemic spreading. On the one hand, our results theoretically confirm the effectiveness of several disinfection strategies. On the other hand, the results provide a basis for making strategic decisions for disinfection schemes.

The organization of the rest paper is as follows. In Sec. II, we first describe the stochastic model of epidemic spreading and then establish numerical models for three types of disinfection strategies. In addition, we also present the epidemic threshold. In Sec. III, we first verify our theoretical results in Sec. II by numerical simulations and then explore the impact of the network structure, the mobility rate of individuals, and the survival rate of pathogens on the prevalence of epidemics. We further compare the three disinfection strategies and give some suggestions for disinfection in reality. In Sec. IV, we summarize the results.

II. INDIRECT TRANSMISSION MODEL ON DIFFERENT DISINFECTION STRATEGIES

A. Stochastic model

Most people have a regular lifestyle and prefer to visit several fixed places, such as supermarkets, workplaces, and schools. Thus, we consider a bipartite network consisting of N individual nodes and M environment nodes ($N \gg M$). Each individual has links with their familiar environments [see Fig. 1(a) for an example]. At each time step, individuals visit each of their familiar environments with probability p, called mobility rate. Here, we assume a uniform mobility rate for the convenience of discussion. Each individual may visit more than one environment at each time step [see Fig. 1(b) for an example]. Individuals are isolated from others if they do not visit any environments, which means they are unable to infect others or get infected. We use matrix $\{a_{ij}\}_{N\times M}$ to represent the bipartite network, where the element $a_{ij} = 1$ if individual node i ($1 \leqslant i \leqslant N$) connects to environment node j ($1 \leqslant j \leqslant M$), otherwise $a_{ij} = 0$.

Disease transmission between two contacting individuals in many epidemic models is simplified as a random event. However, the infection process includes two successive processes for most infectious diseases. As shown in Fig. 2(a), the infected individual will release infectious pathogens, and the susceptible individual may get infected after exposure to those pathogens. For example, a COVID-19 patient releases thousands of novel coronavirus droplets into the air when coughing or sneezing. A healthy person nearby will get infected if the person inhales some droplets into the body and the immune system fails to kill the virus. The disease transmission in a well-mixed group of individuals is similar to the case between two individuals. As shown in Fig. 2(b), infected individuals will release pathogens to the surrounding environment where other susceptible individuals contact the pathogens and get infected with some probability.

In this paper, we assume that each infected visitor will release one unit of pathogens to the environment. At each time step, susceptible individuals will get infected with probability

$$h(\beta) = 1 - (1 - \lambda)^{\beta} \tag{1}$$

after contact $\beta \geqslant 0$ units of pathogens. Infected individuals recover to susceptible ones with probability μ at each time step. When pathogens outside the human body can only survive for a short time, all pathogens in an environment only come from the infected visitors at the current time step. On this condition, our epidemic dynamics has no difference from the classic metapopulation with an SIS process, where the transmission rate is λ.

However, the transmission of epidemics becomes quite different when pathogens can remain infectious for some time. In this scenario, pathogens of environments will come from two resources: residual pathogens from the last time step and

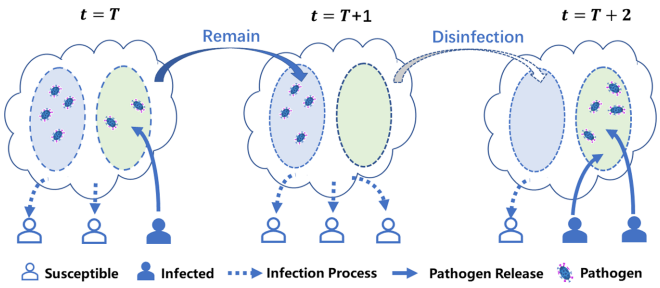

FIG. 3. Time evolution of pathogens in an environment. Pathogens consist of residual pathogens (RP, the left light blue region) and new pathogens (NP, the right light green region). New pathogens at each time step are released by current infected visitors. For example, there are no new pathogens at time $t = T + 1$ because no infected individual visits the environment at time $t = T + 1$. Residual pathogens are left over from the last time step. Since we disinfect the environment at $t = T + 1$, there are no residual pathogens at $t = T + 2$. Disinfecting environment will not influence the disease transmission at the current time step.

new pathogens released by the current infected visitors. For the convenience of discussion, we assume that the proportion γ, called survival rate, of pathogens in environments will remain infectious to the next time step. The survival rate is uniform for all environments. If we define $\tilde{\beta}_j(t)$ as the number of pathogens in environment j at time t, the above process implies

$$\tilde{\beta}_j(t+1) = \gamma\tilde{\beta}_j(t) + n_j(t+1), \tag{2}$$

where $n_j(t)$ is the number of infected visitors of environment j at time t. We call the transmission of disease caused by residual pathogens indirect transmission and that caused by new pathogens direct transmission.

In reality, we can disinfect environments to eliminate their pathogens and reduce indirect transmission. In our model, at the end of each time step, we can disinfect each environment to kill all of its pathogens, which means there are no residual pathogens at the next time step. Equivalently, we can consider that the survival rate is 0 at the disinfection time step. We denote $\gamma_j(t)$, which satisfies

$$\gamma_j(t) = \begin{cases} \gamma, & \text{not disinfect } j \text{ at time } t \\ 0, & \text{disinfect } j \text{ at time } t \end{cases} \tag{3}$$

as the survival rate of pathogens in environment j at time step t. In this way, we rewrite Eq. (2) as

$$\tilde{\beta}_j(t+1) = \gamma_j(t)\tilde{\beta}_j(t) + n_j(t+1) \tag{4}$$

to include the disinfection process. Figure 3 shows the disease transmission process and the role of disinfection in an environment.

In summary, we made three critical assumptions (A1–A3) in the above discussion:

A1. Each infected visitor will release a fixed number of pathogens into the environment.

A2. An environment with β units of pathogens has infectivity as $h(\beta)$.

A3. The evolution process of pathogens in an environment is memoryless or, in other words, a Markov process.

With disinfection not being considered, A1 and A2 are consistent with the classic metapopulation model with an SIS process. A3 means that the number of residual pathogens in an environment only depends on the total pathogens at the last time step, which is intuitive. In addition, A3 is necessary for applying the discrete-Markov method, and a non-Markov process is usually hard to analyze. In fact, the cases are much more complicated in reality than the assumptions and can result in complex phenomena [22]. Since this paper aims to study the impact of indirect transmission and disinfection, simple assumptions without losing much generality will help us focus the research on our interest.

B. Numerical model

Denote $\rho_i(t)$ as the probability of individual i being in the infected state at time t. If individual i is infected at time $t+1$, they are either already infected at time t and have not recovered, or are susceptible at time t and then get infected. So, the formulation of $\rho_i(t+1)$ is

$$\rho_i(t+1) = (1-\mu)\rho_i(t) + (1-\rho_i(t))\pi_i(t), \tag{5}$$

where $\pi_i(t)$ is the probability of susceptible individual i getting infected at time t. Since individual i can be infected when visiting neighboring environments,

$$\pi_i(t) = 1 - \prod_{j=1}^{M}\left(1 - a_{ij}pD_j^i(t)\right), \tag{6}$$

where $D_j^i(t)$ is the conditional probability that environment j infects its susceptible visitor i. However, $h(\tilde{\beta}_j(t))$, which is the infectivity of environment j, will overestimate $D_j^i(t)$ because individual i is known to be susceptible. In fact,

$$n_j(t) = \sum_{s=1}^{N}\boldsymbol{Y}_{sj}(t), \tag{7}$$

according to the definition of $n_j(t)$. $\mathbf{Y}_{sj}(t) = 1$ if individual s is infected and visits environment j at time t; otherwise $\mathbf{Y}_{sj}(t) = 0$. That is,

$$\mathbf{Y}_{sj}(t) \sim \boldsymbol{B}(1, a_{sj}p\rho_s(t)).$$

Thus, by the definition of $D_j^i(t)$,

$$\begin{aligned} D_j^i(t+1) &= E[h(\tilde{\beta}_j(t+1))|\mathbf{Y}_{ij}(t+1) = 0] \\ &= 1 - E[(1-\lambda)^{\gamma_j(t)\tilde{\beta}_j(t)}]E[(1-\lambda)^{\sum_{s\neq i}\mathbf{Y}_{sj}(t+1)}] \\ &= 1 - E[(1-\lambda)^{\gamma_j(t)\tilde{\beta}_j(t)}]\prod_{s\neq i}[1 - a_{sj}p\lambda\rho_s(t+1)]. \end{aligned} \tag{8}$$

Similar to what we do here, in the rest of this paper, we will always neglect the correlation between $n_j(t+1)$ and $\tilde{\beta}_j(t)$, and the correlation among $\{\mathbf{Y}_{sj}(t)\}_{1\leqslant s\leqslant N, 1\leqslant j\leqslant M}$ for each time step t. For simplicity, we note

$$E_j^i(t+1) = \prod_{s\neq i}[1 - a_{sj}p\lambda\rho_s(t+1)] \tag{9}$$

and

$$C_j(t+1) = E[(1-\lambda)^{\gamma_j(t)\tilde{\beta}_j(t)}]. \tag{10}$$

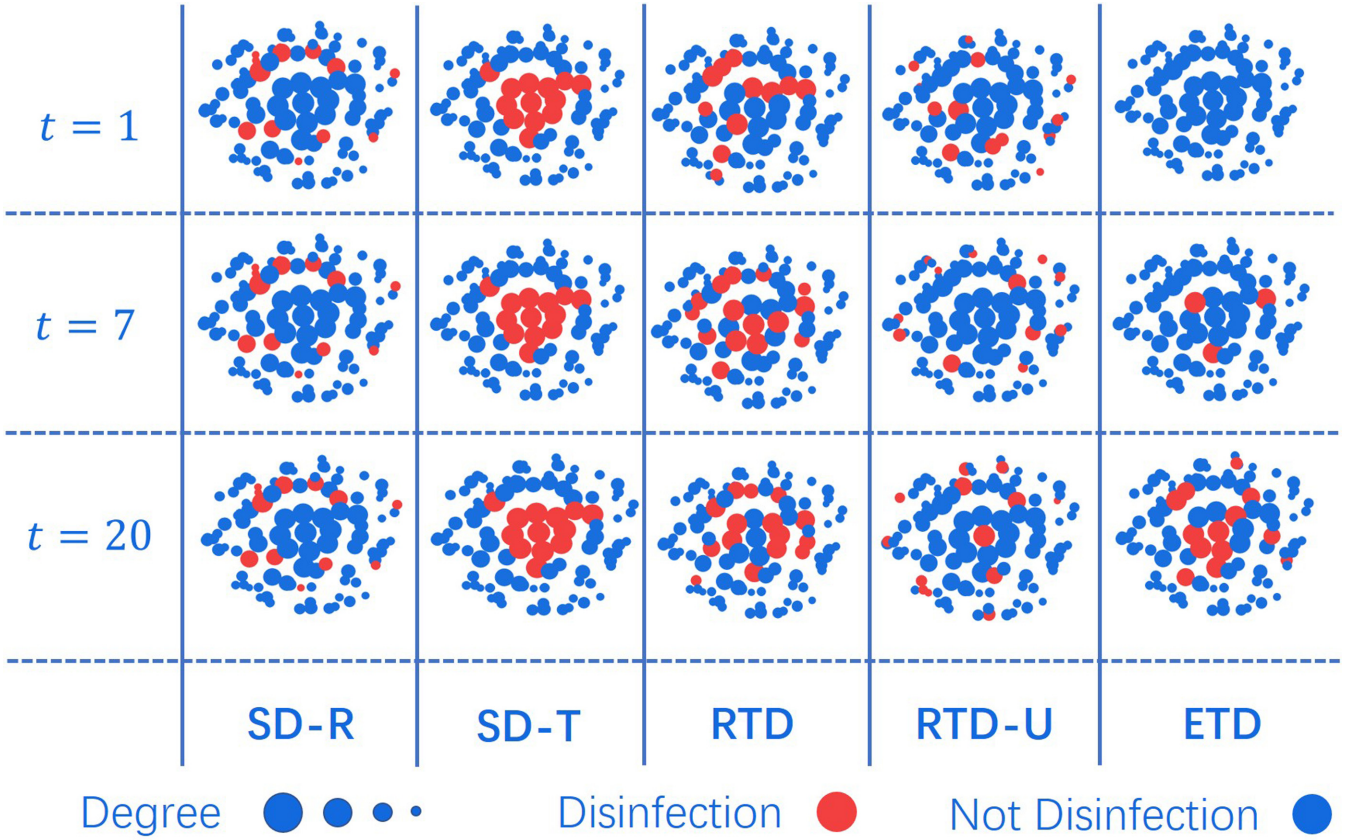

FIG. 4. Disinfection status for 100 environments at three time steps for five disinfection strategies. The results for each disinfection strategy are from a Monte Carlo simulation with $p = 0.25$. In column SD-R, the disinfection environments do not change over time, and they are selected randomly. In column SD-T, the disinfection environments do not change over time and they have the largest degree. In column RTD-U, environments have a uniform probability of being disinfected at each time step. In column RTD, environments have different opportunities to be disinfected. In this example of RTD, environments with a larger degree are more likely to be disinfected. In column ETD, at $t = 1$, few individuals are infected and no environment is disinfected; at $t = 7$, some individuals are infected, which triggers the disinfection of several large-degree environments; at $t = 20$, many individuals are infected and trigger the disinfection of more environments than that at $t = 7$.

Note that $1 - E_j^i(t+1)$ and $1 - C_j(t+1)$ is the probability of getting infected by direct transmission and indirect transmission, respectively.

The disinfection strategy determines the value of $\gamma_j(t)$ and thus has great impact on the distribution of $\tilde{\beta}_j(t)$ in Eq. (4). We propose three disinfection strategies and obtain their $C_j(t)$ in the following.

1. The static disinfection strategy

In the static disinfection strategy (SD), an environment will either be disinfected at every time step or never be disinfected. Denote $\boldsymbol{X} \subseteq \{1, 2, \cdots, M\}$ as the set of environments that we disinfect, SD can be expressed as

$$\gamma_j^{\mathrm{SD}}(t) = \begin{cases} \gamma, & j \notin \boldsymbol{X} \\ 0, & j \in \boldsymbol{X}. \end{cases} \tag{11}$$

The key of SD is the selection of elements in $\boldsymbol{X}$. Inspired by the immunity strategies in Ref. [23], we propose two strategies for selecting environments to be disinfected: Random selection and priority selection of environments with the highest degree. We call the first the static random disinfection strategy (SD-R) and the latter the static target disinfection strategy (SD-T). See Fig. 4 for an example of SD-R and SD-T. We will discuss their efficiency in suppressing epidemic spreading in Sec. III.

To calculate $C_j^{\mathrm{SD}}(t)$, we need to analyze the distribution of $\tilde{\beta}_j^{\mathrm{SD}}(t)$ which relies on $n_j(\tau)$, $\tau \leqslant t$ through Eq. (4). Since $n_j(t)$ is the sum of serveral Bernounlli random variables from Eq. (7), we suppose that $n_j(t)$ approximately satisfies the binomial distribution, which is

$$n_j(t) \sim \boldsymbol{B}(l_j, P_j(t)), \tag{12}$$

where $l_j = \sum_{i=1}^{N} a_{ij}$ is the degree of environment j and

$$P_j(t) = \frac{1}{l_j} \sum_{i=1}^{N} a_{ij} \rho_i(t)$$

is the average probability of all individuals connected to environment j being infected at time t. On the one hand, we find that

$$E[(1-\lambda)^{n_j(t)}] = (1-\lambda)^{E[n_j(t)]} + O(\lambda^2). \tag{13}$$

when Eq. (12) holds and $\lambda \to 0^+$. On the other hand, the number of pathogens in environment $j \notin \boldsymbol{X}$ can be expressed

as

$$\tilde{\beta}_j^{\mathrm{SD}}(t) = \sum_{s=0}^{t-1} \gamma^s n_j(t-s). \tag{14}$$

With Eq. (14), the formulation of $C_j^{\mathrm{SD}}(t)$ becomes

$$C_j^{\mathrm{SD}}(t+1) = \prod_{s=0}^{t-1} E[(1-\lambda)^{\gamma^{s+1} n_j(t-s)}]. \tag{15}$$

By applying Eq. (13) to Eq. (15), we obtain

$$C_j^{\mathrm{SD}}(t+1) = (1-\lambda)^{\gamma E[\tilde{\beta}_j^{\mathrm{SD}}(t)])} + O(\lambda^2). \tag{16}$$

(See Appendix A 1 for more details.) For $j \in \boldsymbol{X}$, we simply have $C_j^{\mathrm{SD}}(t) = 1$.

The time evolution of $E[\tilde{\beta}_j^{\mathrm{SD}}(t)]$ is easy to determine. By taking expectation and using

$$E[n_j(t)] = p \sum_{s=1}^{N} a_{sj} \rho_s(t) \tag{17}$$

in Eq. (4), we obtain

$$\beta_j^{\mathrm{SD}}(t+1) = \gamma_j^{\mathrm{SD}}(t) \beta_j^{\mathrm{SD}}(t) + \sum_{s=1}^{N} a_{sj} p \rho_s(t+1), \tag{18}$$

where we note $\beta_j^{\mathrm{SD}}(t) = E[\tilde{\beta}_j^{\mathrm{SD}}(t)]$ for convenience. With Eqs. (16) and (18), we finally establish a solvable numerical model for SD.

2. The random time disinfection strategy

The second type of disinfection strategies is the random time disinfection strategy (RTD). At each time step, we independently disinfect each environment j with probability u_j. When all environments have the same disinfection probability, that is $u_j = u$, $0 \leqslant u \leqslant 1$, $\forall j \in \{1, 2, \cdots, M\}$, we call it the uniform random time disinfection strategy (RTD-U). See Fig. 4 for an example of RTD-U and RTD. In RTD, $\gamma_j^{\mathrm{RTD}}(t)$ is a random variable following the distribution

$$\boldsymbol{P}\big(\gamma_j^{\mathrm{RTD}}(t) = x\big) = \begin{cases} u_j, & x = 0 \\ 1 - u_j, & x = \gamma, \end{cases}$$

which is time independent.

When the spreading process is stable and Eq. (12) holds, we prove in Appendix A 2 that

$$C_j^{\mathrm{RTD}}(t) = u_j + (1-u_j)\phi((1-\lambda)^{\gamma \beta_j^{\mathrm{RTD}}(t)}, u_j, \gamma) + O(\lambda^2), \tag{19}$$

where

$$\phi(x, u, \gamma) = \frac{u}{1-u} \sum_{s=1}^{\infty} (1-u)^s x^{\frac{1-\gamma+\gamma u}{1-\gamma}(1-\gamma^{s+1})}. \tag{20}$$

Finally, by taking expectation in Eq. (4), we have

$$\beta_j^{\mathrm{RTD}}(t+1) = (1-u_j)\gamma \beta_j^{\mathrm{RTD}}(t) + \sum_{s=1}^{N} a_{sj} p \rho_s(t+1). \tag{21}$$

3. The event-trigger disinfection strategy

Inspired by the terminal disinfection commonly adopted in containment of epidemics, we introduce the event-triggered disinfection strategy (ETD). We disinfect environment j at time t only when the number of its infected visitors reaches a given threshold $n_c \in \mathbb{N}$. See Fig. 4 for an example of ETD. Thus,

$$\gamma_j^{\mathrm{ETD}}(t) = \begin{cases} \gamma, & n_j(t) \leqslant n_c \\ 0, & n_j(t) > n_c \end{cases} \tag{22}$$

in ETD.

Since $n_j(\tau) \leqslant n_c$ for all τ, we have

$$\gamma_j^{\mathrm{ETD}}(t) \tilde{\beta}_j^{\mathrm{ETD}}(t) \leqslant \frac{\gamma}{1-\gamma} n_c. \tag{23}$$

Thus, when n_c is small enough,

$$\begin{aligned} C_j^{\mathrm{ETD}}(t) &= E\big[(1-\lambda)^{\gamma_j^{\mathrm{ETD}}(t)\tilde{\beta}_j^{\mathrm{ETD}}(t)}\big] \\ &\approx 1 - \lambda E\big[\gamma_j^{\mathrm{ETD}}(t)\tilde{\beta}_j^{\mathrm{ETD}}(t)\big] \\ &\approx (1-\lambda)^{E[\gamma_j^{\mathrm{ETD}}(t)\tilde{\beta}_j^{\mathrm{ETD}}(t)]}. \end{aligned} \tag{24}$$

In Appendix A 3, we prove that

$$C_j^{\mathrm{ETD}}(t+1) = (1-\lambda)^{E[\gamma_j^{\mathrm{ETD}}(t)\tilde{\beta}_j^{\mathrm{ETD}}(t)]} + O\big(n_c^2 \lambda^2\big). \tag{25}$$

Similar to $E[\tilde{\beta}_j^{\mathrm{SD}}(t)]$, the time evolution function of $E[\gamma_j^{\mathrm{ETD}}(t)\tilde{\beta}_j^{\mathrm{ETD}}(t)]$ can be easily obtained from Eq. (4). When Eq. (12) holds, the probability of not disinfecting environment j at time t is

$$q_j(t) = \sum_{s=0}^{n_c} \binom{l_j}{s} P_j(t)^s (1 - P_j(t))^{l_j - s}. \tag{26}$$

By multiplying both sides of

$$\tilde{\beta}_j^{\mathrm{ETD}}(t) = \gamma_j(t-1)\tilde{\beta}_j^{\mathrm{ETD}}(t-1) + n_j(t) \tag{27}$$

by $\gamma_j^{\mathrm{ETD}}(t)$ and taking expectation, we obtain

$$\begin{aligned} \theta_j^{\mathrm{ETD}}(t+1) &= \gamma q_j(t) \theta_j^{\mathrm{ETD}}(t) \\ &+ \gamma \textstyle\sum_{s=0}^{n_c} P_j(t)^s (1 - P_j(t))^{l_j - s} s, \end{aligned} \tag{28}$$

where $\tilde{\theta}_j^{\mathrm{ETD}}(t+1) = \gamma_j^{\mathrm{ETD}}(t)\tilde{\beta}_j^{\mathrm{ETD}}(t)$ and $\theta_j^{\mathrm{ETD}}(t) = E[\tilde{\theta}_j^{\mathrm{ETD}}(t)]$. In fact, $\tilde{\theta}_j^{\mathrm{ETD}}(t)$ represents the number of residual pathogens in environment j at time t.

C. Epidemic threshold

We obtain the epidemic threshold by analyzing the stability of the disease-free equilibrium. Although the three types of disinfection strategies proposed above have various expressions, they possess the same linearized form near the disease-free equilibrium (See Appendix B for detailed derivation of the threshold expression). Thus, SD, RTD, and ETD have the same threshold expression as

$$\lambda_{\max}(-\mu \boldsymbol{I}_N + p^2 \lambda [\boldsymbol{K} - \boldsymbol{A}(\boldsymbol{G}_0 - \boldsymbol{I}_M)^{-1} \boldsymbol{G}_0 \boldsymbol{A}^{\mathrm{T}}]) < 0, \tag{29}$$

where $(\boldsymbol{K})_{ss} = 0$, $(\boldsymbol{K})_{sl} = (\boldsymbol{A}\boldsymbol{A}^{\mathrm{T}})_{sl}$, $\forall 1 \leqslant s \neq l \leqslant N$ and $\boldsymbol{G}_0 = \mathrm{diag}(\gamma_1, \gamma_2, \cdots, \gamma_M)$. The only difference of the threshold expression among disinfection strategies is the value of $\boldsymbol{G}_0$. For SD, $\gamma_j = \gamma$ if $j \in \boldsymbol{X}$; otherwise, $\gamma_j = 0$. For RTD, $\gamma_j = (1-u_j)\gamma$, $1 \leqslant j \leqslant M$ according to Eq. (21). As

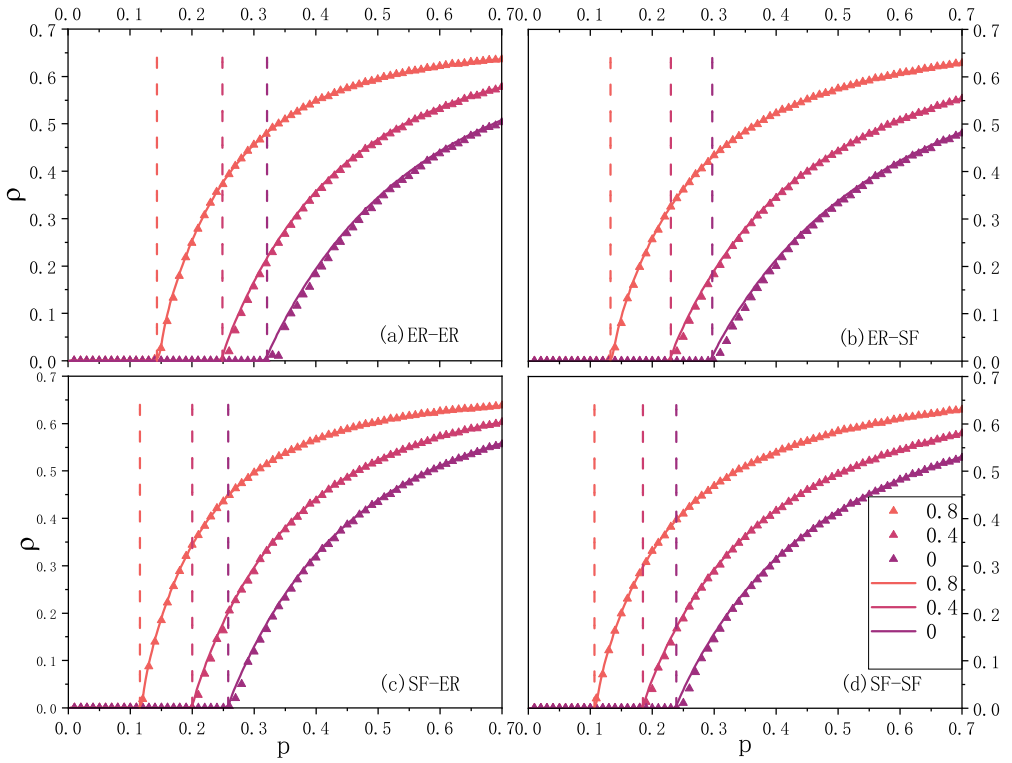

FIG. 5. The prevalence ρ without disinfection ($\boldsymbol{X} = \emptyset$) as a function of mobility rate p on (a) ER-ER network, (b) ER-SF network, (c) SF-ER network, and (d) SF-SF network. Triangles are the average results of 20 independent Monte Carlo simulations, and solid lines are the results of numerical model obtained in Sec. II B 1. Vertical dotted lines are the theoretical threshold obtained by Eq. (29). Simulations are carried out when the survival rate γ is 0, 0.4, and 0.8.

ETD only disinfects environments when the epidemic has outbroken, it has the same threshold as that for the condition without disinfection, which means $\gamma_j = \gamma, 1 \leqslant j \leqslant M$ for ETD.

III. NUMERICAL SIMULATIONS AND ANALYSIS

A. Impacts of network structures and model parameters without disinfection

To verify the theoretical results obtained in the previous section, we carry out Monte Carlo simulations on networks with $N = 1000, M = 100$, and 4000 edges. The network structure significantly impacts the dynamic behavior of epidemic spreading [24–26], so we apply different networks in our simulations. Since our network is a bipartite graph, we first give degree sequences of environment nodes and individual nodes and then generate a configuration model network. Specifically, we use two degree sequences for each node type, following the power-law distribution and Poisson distribution, and generate four networks by the pairwise combination of degree sequences. If the degree sequences of environment nodes and individual nodes follow the power-law distribution and Poisson distribution, respectively, we call this network the SF-ER network. In the same way, we name the other three networks the SF-SF, ER-SF, and ER-ER networks.

In the following discussion, we fix $\mu = 0.5, \lambda = 0.02$ and only consider the impact of p and γ on the spreading process. For the four networks and different values of γ, we compare the theoretical results with Monte Carlo simulations in Fig. 5, which show perfect agreement. It is worth noting that no indirect transmission occurring in environments when the survival rate $\gamma = 0$. Thus, the indirect transmission brings the prevalence gap between curves of $\gamma = 0$ and $\gamma \neq 0$. The prevalence of epidemics ρ is defined as

$$\rho = \lim_{t\to\infty} \frac{1}{N} \sum_{i=1}^{N} \rho_i(t).$$

Figure 5 shows indirect transmission will significantly increase the prevalence ρ. By comparing the subgraphs in the same row or column in Fig. 5, we demonstrate that the network with the power-law distribution has a smaller threshold than the one with Poisson distribution, regardless of environment nodes or individual nodes. The SF-SF network has the smallest threshold.

To verify the threshold expression Eq. (29), we proceed with Monte Carlo simulations on various values of p and γ in Fig. 6. The theoretical threshold (red lines) agrees well with the boundary of the disease-free region (yellow regions) in the phase diagram. The threshold of mobility rate declines with the increase of γ. When $\gamma = 1$, the number of pathogens will not decay over time but accumulate infinitely. Even a small mobility rate p will lead to an epidemic outbreak in this situation. That is, the threshold of p is 0.

Considering the practical implications of our model, we conclude that the risk of a large-scale epidemic outbreak will increase when pathogens are easy to remain infectious in

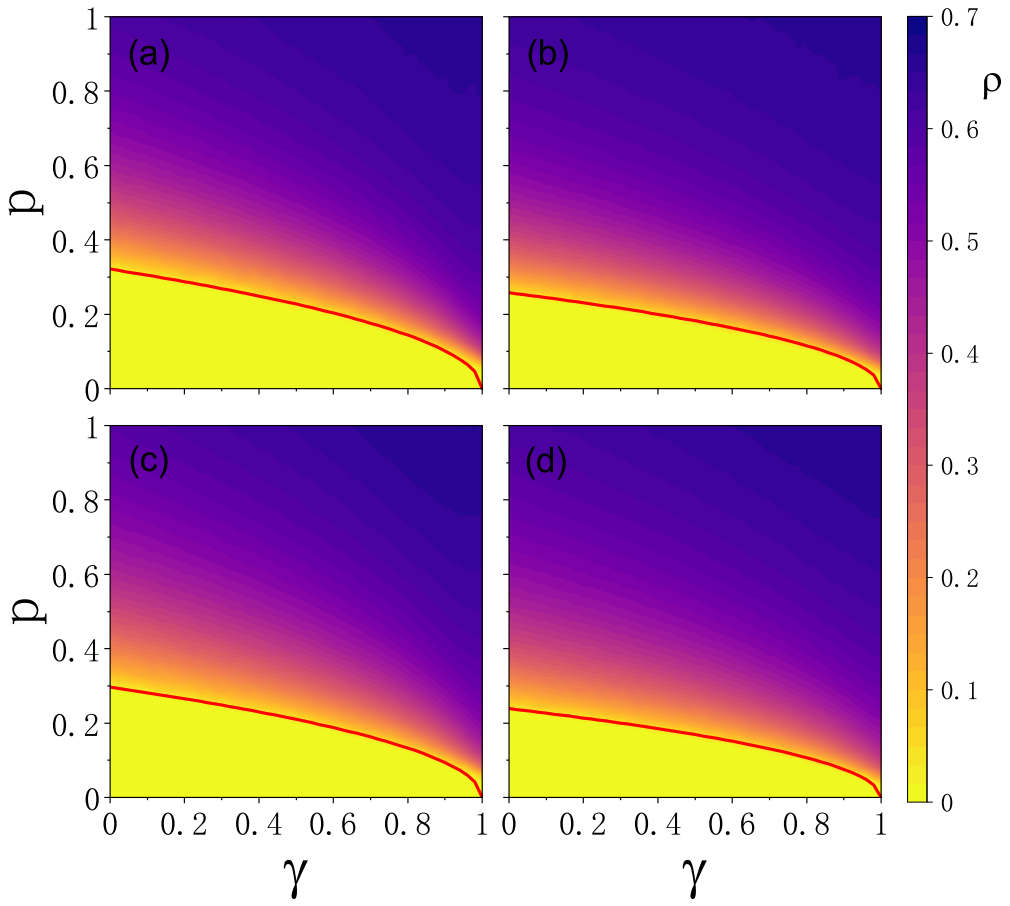

FIG. 6. Phase diagram for the prevalence ρ average on 20 independent simulations without disinfection ($\boldsymbol{X} = \emptyset$) under different values of p and γ. The results are obtained on (a) ER-ER network, (b) ER-SF network, (c) SF-ER network, and (d) SF-SF network. Red solid lines are the theoretical thresholds obtained by Eq. (29).

environments. This conclusion confirms the necessity and the importance of disinfection in reality.

B. Comparative analysis of different disinfection strategies

In the following part, to find out the critical factors of disinfection strategies, we will discuss the efficiency of five disinfection strategies: SD-R, SD-T, RTD-U, RTD, and ETD. To judge their efficiency in containing epidemics, we compare the prevalence ρ when they have the same cost of disinfection resources. We quantify the disinfection resources used for environment j by its disinfection frequency, which is defined as

$$F_j = \lim_{T\to\infty} \frac{1}{T} \sum_{t=0}^{T} \delta_{\gamma(t),0}, \tag{30}$$

where

$$\delta_{x,y} = \begin{cases} 1, & x = y \\ 0, & x \neq y. \end{cases}$$

Furthermore, we take the average frequency

$$AF = \frac{1}{M} \sum_{j=1}^{M} F_j$$

to measure the average disinfection resources used for all environments. The two indices, F_j and AF, are calculated for different disinfection strategies.

We start by comparing the efficiency of SD-R, SD-T, RTD-U. On the one hand, Fig. 7(a) clearly shows that SD-T has the smallest prevalence and SD-R has the largest prevalence among the three strategies for the same level of AF. On the other hand, Fig. 7(b) shows that for the mobility rate, SD-T has a greater threshold than RTD-U and RTD-U has a greater threshold than SD-R. Thus, on containing epidemics, the efficiency of SD-T, RTD-U, and SD-R is a decreasing sequence.

The analysis above suggests that the management should prioritize disinfection to environments with large visitor flow. When the visitor flow of environments is unknown (that is, we can not know the degree of environment nodes), it is better to allocate resources to all environments than only some of them.

Since Fig. 7 demonstrates that SD-T performs better than SD-R and RTD-U, we only need to compare SD-T, RTD, and ETD in the following. However, we want to show some basic features of ETD before the comparison. ETD better reflects the complexity of the disinfection strategy than SD and RTD. Both SD and RTD focus on the spatial allocation of disinfection resources to environments and act homogeneously on the time dimension. However, ETD is a dynamic strategy associated with the spreading process of epidemics.

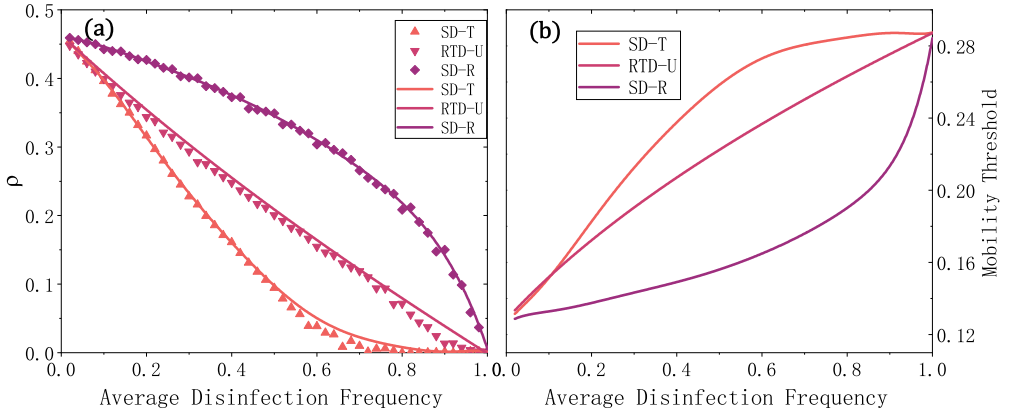

FIG. 7. (a) Epidemic prevalence ρ and (b) the mobility threshold varying with the average disinfection frequency (AF) for the three disinfection strategies. Solid lines represent the theoretical results, and the scatters are results averaged over 20 independent simulations on the SF-ER network with $\gamma = 0.8$. The mobility rate in (a) is fixed as the theoretical threshold when $AF = 1$. Each simulation of SD-R is conducted on 25 different selections of $\boldsymbol{X}$.

In Fig. 8, we investigate the prevalence ρ varying with the mobility rate p for different trigger thresholds n_c. In Fig 8(a), curves $n_c = 1, 2, 4$ are sandwiched between curves $n_c = 0$ and $n_c = \infty$ and asymptotically approach to the former with the increase of p. It is easy to understand as the number of infected visitors and the disinfection frequency of environments will simultaneously increase with the mobility rate p.

Figure 8(b) clearly shows that the disinfection frequencies of environments are positively correlated to the mobility rate and their degrees. In Fig. 8(a), curve $n_c = 1$ is significantly lower than curve $n_c = \infty$ when $p = 0.2$. Figure 8(b) shows that AF is small when $p = 0.2$. Therefore, we demonstrate that when p is small, ETD can significantly reduce the prevalence ρ at a small AF, which implies a low cost in disinfection resources.

When $p = 0.3$, curves $n_c = 1$ and $n_c = 0$ in FIG. 8(a) are very close. However, FIG. 8(b) shows that there are still many environments with both low degree and low disinfection frequencies when $p = 0.3$. This investigation proves once again that the disinfection of environments with larger visitor flow is essential for suppressing epidemic spreading.

As shown in Fig. 9, RTD is significantly superior to SD-T. It is intuitive that if disinfection resources are only allocated to large-degree environments as SD-T does, there will be many pathogens in low-degree environments. Instead, allocating parts of disinfection resources to low-degree environments reduces the number of their pathogens. At the same time, it will not bring much increment to large-degree environments, which is ultimately more conducive to suppressing epidemic spreading.

Although RTD and ETD have the same F_j ($1 \leqslant j \leqslant M$), ETD always performs better than RTD in Fig. 9, for ETD has a better strategy than RTD on the time dimension. In general, ETD can allocate disinfection resources efficiently on both spatial and time dimensions in the case of limited resources.

In Figs. 9(c) and 9(d), we find that the disinfection frequencies of environments are low when the prevalence gap between RTD (or SD-T) and ETD in Figs. 9(a) and 9(b) reaches its maximum. Therefore, ETD is more cost effective than RTD and SD-T, especially when disinfection resources are insufficient.

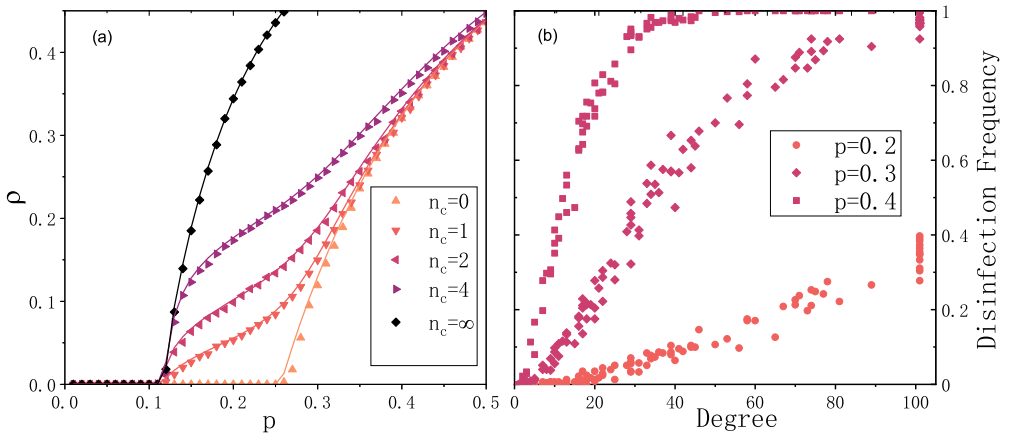

FIG. 8. (a) The prevalence ρ under ETD as a function of mobility rate p for trigger thresholds $n_c = 0, 1, 2, 4, \infty$. Scatters are average results of 20 independent simulations and solid lines are theoretical results. Simulations are carried out on the SF-ER network and $\gamma = 0.8$. In particular, $n_c = \infty$ will lead to $AF = 0$ and $n_c = 0$ will lead to no residual pathogens in environments. (b) The relation of degree l_j and disinfection frequency F_j for all environments j when $n_c = 1$ with different mobility rates $p = 0.2, 0, 3, 0.4$.

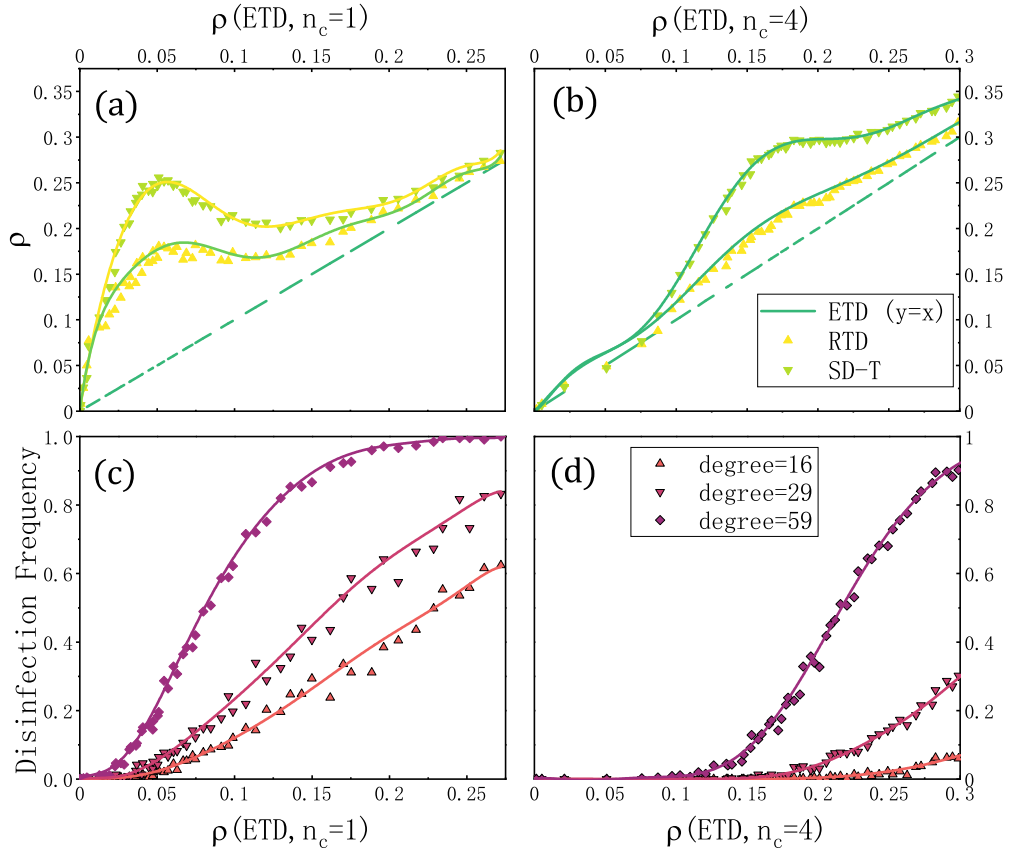

FIG. 9. Comparison of SD-T, RTD, and ETD average on 20 independent simulations on the SF-ER network with trigger thresholds as (a) $n_c = 1$ and (b) $n_c = 4$. For the scatters in (a) and (b), the horizontal values are the prevalence ρ of ETD, and the vertical values are the prevalence of RTD (or SD-T) with the same F_j, $1 \leqslant j \leqslant M$ (or AF) as ETD. The solid lines are theoretical results. (c) and (d) show the disinfection frequencies for three environments with their degree as 16,29,59, respectively. There are 25%, 50%, and 75% of environments with degree lower than 16,29, and 59, respectively. The solid lines in (c) and (d) are theoretical results obtained from Eq. (26). To draw this figure, we first record the environments' disinfection frequencies in ETD when doing simulations with various mobility rates. Then, under the same disinfection frequencies (or average disinfection frequency) as ETD, we obtain the prevalence ρ of RTD (or SD-T) by Monte Carlo simulations and finally summarize all results to form this figure. Note that we use the prevalence ρ in ETD, instead of mobility rates, as the horizontal coordinate.

IV. CONCLUSION

In this paper, we modeled the indirect transmission where environments can infect their visitors. We first demonstrated that both indirect transmission and heterogeneous networks facilitate epidemic spreading. Then, we considered disinfection and studied the efficiency of the static disinfection strategy, the RTD strategy, and the event-triggered disinfection strategy. We obtained the threshold of the epidemic outbreak and provided insights on the allocation of disinfection resources to prevent epidemics. Based on the comparative analysis of the three disinfection strategies on the heterogeneous network, we found that environments with more visitors should be allocated with more disinfection resources. Meanwhile, we discovered that disinfecting environments with few visitors is necessary to suppress epidemic spreading. Studies about ETD confirm that the timely disinfection of environments with infected visitors is effective and economical.

In a word, we have conducted an initial study on indirect transmission and the disinfection strategy. Besides these simple and basic disinfection strategies, we have provided some theoretical support for epidemics prevention and control measures.

ACKNOWLEDGMENTS

This work is supported in part by the National Key Research and Development Program of China under Grant No. 2018AAA0101100, in part by the National Natural Science Foundation of China under Grant No. 61973241, and in part by the Natural Science Foundation of Jiangsu Province under Grant No. BK20220678. The numerical calculations in this paper have been done on the supercomputing system in the Supercomputing Center of Wuhan University.

APPENDIX A: THE APPROXIMATION OF $C_j(t)$

In Sec. II B 1, we roughly described the derivation of $C_j^{\mathrm{SD}}(t)$, $C_j^{\mathrm{RTD}}(t)$, and $C_j^{\mathrm{ETD}}(t)$ for brevity. This Appendix will provide the details of how to get the approximations.

First, we redeclare the problems we need to solve here. Taking $C_j^{\mathrm{SD}}(t)$, for example, we obtain in the text that

$$C_j^{\mathrm{SD}}(t) = E[(1-\lambda)^{\gamma \tilde{\beta}_j^{\mathrm{SD}}(t)}], \tag{A1}$$

where

$$\tilde{\beta}_j^{\mathrm{SD}} = \sum_{s=0}^{t-1} \gamma^s n_j(t-s). \tag{A2}$$

In the text, we explain that $n_j(t)$ approximately satisfies a Bernoulli distribution, which is

$$n_j(t) \sim \boldsymbol{B}(l_j, P_j(t)), \tag{A3}$$

where

$$P_j(t) = \frac{1}{l_j} \sum_{i=1}^{N} a_{ij}\rho_i(t).$$

Since our system is an SIS process, the distribution of $n_j(t)$ will reach an stable state when t is large enough. From Eqs. (A3) and (A2), it is easy to know that $\beta_j^{\mathrm{SD}}(t) = E[\tilde{\beta}_j^{\mathrm{SD}}(t)]$ is the scale parameter of the distribution of $\tilde{\beta}_j^{\mathrm{SD}}(t)$ when the spreading process is stable. Thus, $C_j^{\mathrm{SD}}(t)$ must be an function of $\beta_j^{\mathrm{SD}}(t)$ from Eq. (A1). Our purpose is to find an approximation of this function. Similarly, we want to find the relations between $C_j^{\mathrm{RTD}}(t)$, $C_j^{\mathrm{ETD}}(t)$ and $\beta_j^{\mathrm{RTD}}(t)$, $\beta_j^{\mathrm{ETD}}(t)$, respectively.

For the sake of further discussion, we introduce three important conclusions here.

Lemma 1. If $\boldsymbol{X} \sim \boldsymbol{B}(n, p)$ and $0 < \lambda, s < 1$, then

$$|E[(1-\lambda)^{s\boldsymbol{X}}] - (1-\lambda)^{sE[\boldsymbol{X}]}| < nps\lambda^2$$

Proof. Since

$$\begin{aligned} &E[(1-\lambda)^{s\boldsymbol{X}}] \\ &= \textstyle\sum_{k=0}^{n}(1-\lambda)^{sk}\binom{n}{k}p^k(1-p)^{n-k} \\ &= \textstyle\sum_{k=0}^{n}\binom{n}{k}[p(1-\lambda)^s]^k(1-p)^{n-k} \\ &= [p(1-\lambda)^s + 1 - p]^n \end{aligned}$$

and

$$(1-\lambda)^{sE[\boldsymbol{X}]} = (1-\lambda)^{snp},$$

we have

$$\begin{aligned} &|E[(1-\lambda)^{s\boldsymbol{X}}] - (1-\lambda)^{sE[\boldsymbol{X}]}| \\ &= |[p(1-\lambda)^s + 1 - p]^n - [(1-\lambda)^{sp}]^n| \\ &< n[p(1-\lambda)^s + 1 - p - (1-\lambda)^{sp}]. \end{aligned}$$

Note

$$g(\lambda) = p(1-\lambda)^s + 1 - p - (1-\lambda)^{sp}.$$

It is easy to find that

$$\begin{aligned} g(0) &= 0, \\ g'(0) &= 0, \\ g''(\lambda) &< 2ps. \end{aligned}$$

According to the Taylor expansion of $g(\lambda)$ with a Lagrange remainder, we obatin

$$g(\lambda) < ps\lambda^2,$$

which means

$$|E[(1-\lambda)^{s\boldsymbol{X}}] - (1-\lambda)^{sE[\boldsymbol{X}]}| < nps\lambda^2.$$

Lemma 2. If $0 < a_i, b_i < 1$ and $|a_i - b_i| < \epsilon_i$, $1 < i < n$, then

$$\left|\prod_{i=1}^{n} a_i - \prod_{i=1}^{n} b_i\right| < \sum_{i=1}^{n} \epsilon_i.$$

We omit the proof of Lemma 2 here.

Lemma 3. If positive random variable $\boldsymbol{X} \leqslant a$ and $0 < \lambda < 1$, then

$$|E[(1-\lambda)^{\boldsymbol{X}}] - (1-\lambda)^{E[\boldsymbol{X}]}| < \max\left\{\frac{1}{4}, a^2\right\}\frac{\lambda^2}{(1-\lambda)^2}.$$

Proof. Notice that

$$(1-\lambda)^y = 1 - y\lambda + y(y-1)(1-\xi)^{y-2}\frac{\lambda^2}{2}$$

for arbitrary y, where $0 < \xi < \lambda$ is a function of y. On the one hand, since $\boldsymbol{X}(\boldsymbol{X}-\boldsymbol{1}) < \max\{\frac{1}{4}, a^2\}$ and $(1-\xi)^{\boldsymbol{X}-2} < (1-\lambda)^{-2}$,

$$|E[(1-\lambda)^{\boldsymbol{X}}] - 1 + \lambda E[\boldsymbol{X}]| < \max\left\{\frac{1}{4}, a^2\right\}\frac{\lambda^2}{2(1-\lambda)^2}.$$

On the other hand, we have $E[\boldsymbol{X}] < a$, therefore

$$|(1-\lambda)^{E[\boldsymbol{X}]} - 1 + \lambda E[\boldsymbol{X}]| < \max\left\{\frac{1}{4}, a^2\right\}\frac{\lambda^2}{2(1-\lambda)^2}.$$

■

In conclusion,

$$|E[(1-\lambda)^{\boldsymbol{X}}] - (1-\lambda)^{E[\boldsymbol{X}]}| < \max\left\{\frac{1}{4}, a^2\right\}\frac{\lambda^2}{(1-\lambda)^2}.$$

Since $\lambda = 0.02$ in our simulations, we treat λ as a number close to 0 in the following analysis.

1. Derivation of $C_j^{\mathrm{SD}}(t)$

For SD, $\tilde{\beta}_j(t) = 0$ for $j \notin \boldsymbol{X}$. For $j \in \boldsymbol{X}$,

$$\tilde{\beta}_j^{\mathrm{SD}}(t) = \sum_{s=0}^{t-1} \gamma^s n_j(t-s). \tag{A4}$$

Assuming $n_j(\tau)$, $1 < \tau < t$ are independent, we can further obtain that

$$\begin{aligned} C_j^{\mathrm{SD}}(t+1) &= E[(1-\lambda)^{\gamma\sum_{s=0}^{t-1}\gamma^s n_j(t-s)}] \\ &= \prod_{s=0}^{t-1} E[(1-\lambda)^{\gamma^{s+1}n_j(t-s)}]. \end{aligned} \tag{A5}$$

By applying Lemmas 1 and 2, we have

$$\begin{aligned} &\left|C_j^{\mathrm{SD}}(t+1) - (1-\lambda)^{\gamma\beta_j^{\mathrm{SD}}(t)}\right| \\ &= \left|\prod_{s=0}^{t-1} E[(1-\lambda)^{\gamma^{s+1}n_j(t-s)}] - \prod_{s=0}^{t-1}(1-\lambda)^{\gamma^{s+1}E[n_j(t-s)]}\right| \\ &< \sum_{s=0}^{t-1} |E[(1-\lambda)^{\gamma^{s+1}n_j(t-s)}] - (1-\lambda)^{\gamma^{s+1}E[n_j(t-s)]}| \\ &< \sum_{s=0}^{t-1} \gamma^{s+1} l_j P_j(t-s)\lambda^2 < \sum_{s=0}^{t-1} l_j\gamma^{s+1}\lambda^2 < \frac{\gamma l_j}{1-\gamma}\lambda^2, \end{aligned} \tag{A6}$$

which means

$$C_j^{\mathrm{SD}}(t+1) = (1-\lambda)^{\gamma\beta_j^{\mathrm{SD}}(t)} + \boldsymbol{O}(\lambda^2).$$

2. Derivation of $C_j^{\mathrm{RTD}}(t)$

In RTD, if the last time we disinfect environment j is at time step $t-s$ ($s \geqslant 1$), the number of pathogens at the current time step t is $\sum_{k=0}^{s-1}\gamma^k n_j(t-k)$, which happens with probability $(1-u_j)^{s-1}u_j$. Thus,

$$\begin{aligned} &C_j^{\mathrm{RTD}}(t+1) \\ &= E[(1-\lambda)^{\gamma_j^{\mathrm{RTD}}(t)\tilde{\beta}_j^{\mathrm{RTD}}(t)}] \\ &= u_j + (1-u_j)E[(1-\lambda)^{\gamma\tilde{\beta}_j^{\mathrm{RTD}}(t)}] \\ &= u_j + \sum_{s=1}^{t}(1-u_j)^s u_j E[(1-\lambda)^{\sum_{k=0}^{s-1}\gamma^{k+1}n_j(t-k)}]. \end{aligned} \tag{A7}$$

Similar to Eq. (A6), for every term in Eq. (A7), we have

$$\begin{aligned} &\left|E[(1-\lambda)^{\sum_{k=0}^{s-1}\gamma^{k+1}n_j(t-k)}] - (1-\lambda)^{\sum_{k=0}^{s-1}\gamma^{k+1}E[n_j(t-k)]}\right| \\ &< \frac{\gamma-\gamma^{s+1}}{1-\gamma}l_j\lambda^2 < \frac{\gamma l_j}{1-\gamma}\lambda^2. \end{aligned}$$

Thus,

$$\begin{aligned} &C_j^{\mathrm{RTD}}(t+1) \\ &= u_j + \textstyle\sum_{s=1}^{t}(1-u_j)^s u_j(1-\lambda)^{\sum_{k=0}^{s-1}\gamma^{k+1}E[n_j(t-k)]} + R \end{aligned} \tag{A8}$$

and $|R| < (1-u_j)\frac{\gamma l_j}{1-\gamma}\lambda^2$.

Unfortunately, it is hard to further simplify Eq. (A8) to make $C_j^{\mathrm{RTD}}(t)$ a function of $\beta_j^{\mathrm{RTD}}(t)$. As we have discussed before, we can be sure that $C_j^{\mathrm{RTD}}(t+1)$ is a function of $\beta_j(t)$ only when the spreading process reaches the stable state. Since we are mainly interested in the equilibrium of an SIS process, we give the iteration method of getting the equilibrium for ETD in the following. In the stable state, we denote

$$P_j = \frac{1}{l_j}\sum_{i=1}^{N} a_{ij}\rho_i$$

as the average probability of individuals connected to environment j in an infected state. On the one hand, if at time step τ, the spreading process is stable, then

$$n_j(\tau) \sim \boldsymbol{B}(l_j, P_j). \tag{A9}$$

On the other hand, the value of $\beta_j^{\mathrm{RTD}}(t)$ is dominated by the $n_j(t-k)$ where k is small compared to t. Thus,

$$\sum_{k=0}^{s-1}\gamma^{k+1}E[n_j(t-k)] = \frac{\gamma(1-\gamma^{s+1})}{1-\gamma}P_j l_j \tag{A10}$$

and

$$\beta_j^{\mathrm{RTD}}(t) = \sum_{s=0}^{t}(1-u_j)^s\gamma^s E[n_j(t-s)] = \frac{P_j l_j}{1-(1-u_j)\gamma} \tag{A11}$$

when t is large enough for the spreading process to be stable. From Eqs. (A11) and (A10),

$$\sum_{k=0}^{s-1}\gamma^{k+1}E[n_j(t-k)] = \frac{\gamma(1-\gamma+u_j\gamma)}{1-\gamma}(1-\gamma^{s+1})\beta_j^{\mathrm{RTD}}(t) \tag{A12}$$

holds when t is large enough. If we note

$$\phi(x,u,\gamma) = \frac{u}{1-u}\sum_{s=1}^{\infty}(1-u)^s x^{\frac{1-\gamma-\gamma u}{1-\gamma}(1-\gamma^{s+1})}$$

and use Eq. (A12), Eq. (A8) becomes

$$C_j^{\mathrm{RTD}}(t+1) = u_j + (1-u_j)\phi((1-\lambda)^{\gamma\beta_j^{\mathrm{RTD}}(t)}, u_j, \gamma) + R. \tag{A13}$$

Notice that $C_j^{\mathrm{RTD}}(t+1)$ is now a function of $\beta_j^{\mathrm{RTD}}(t)$. Even though Eq. (A13) only holds when t is large enough, on which condition the spreading process is stable, we find it works well on obtaining the equilibrium by iteration.

3. Derivation of C_j^{ETD}

We obtain in the text that

$$\tilde{\beta}_j^{\mathrm{ETD}}(t) = \gamma_j^{\mathrm{ETD}}(t-1)\tilde{\beta}_j^{\mathrm{ETD}}(t-1) + n_j(t)$$

and define $\tilde{\theta}_j^{\mathrm{ETD}}(t+1) = \gamma_j^{\mathrm{ETD}}(t)\tilde{\beta}_j^{\mathrm{ETD}}(t)$, where

$$\gamma_j^{\mathrm{ETD}}(t) = \begin{cases} \gamma, & n_j(t) \leqslant n_c \\ 0, & n_j(t) > n_c. \end{cases}$$

Thus,

$$\tilde{\theta}_j^{\mathrm{ETD}}(t+1) = \gamma_j^{\mathrm{ETD}}(t)\tilde{\theta}_j^{\mathrm{ETD}}(t) + \gamma_j^{\mathrm{ETD}}(t)n_j(t).$$

It is obviously that $\tilde{\theta}^{\mathrm{ETD}}(t+1) \leqslant \gamma\tilde{\theta}_j^{\mathrm{ETD}}(t) + \gamma n_c$ from the above equation, which indicates that

$$\tilde{\theta}_j^{\mathrm{ETD}}(t) \leqslant \frac{\gamma n_c}{1-\gamma}. \tag{A14}$$

Since

$$C_j^{\mathrm{ETD}}(t) = E[(1-\lambda)^{\tilde{\theta}_j^{\mathrm{ETD}}(t)}],$$

by applying Lemma 3, we have

$$\left|C_j^{\mathrm{ETD}}(t) - (1-\lambda)^{E[\tilde{\theta}_j^{\mathrm{ETD}}(t)]}\right| < \max\left\{\frac{1}{4}, \left(\frac{\gamma n_c}{1-\gamma}\right)^2\right\}\frac{\lambda^2}{(1-\lambda)^2},$$

which means

$$C_j^{\mathrm{ETD}}(t) = (1-\lambda)^{E[\tilde{\theta}_j^{\mathrm{ETD}}(t)]} + \boldsymbol{O}\left(n_c^2\lambda^2\right).$$

APPENDIX B: DERIVATION OF THRESHOLD EXPRESSION

Since $\rho_i(t) \ll 1$, $\beta_j(t) \ll 1$ near the disease-free equilibrium, we have approximation

$$\begin{aligned} D_j^i(t) &\approx \lambda\gamma_j\beta_j(t-1) + \sum_{s\neq i} a_{sj}\lambda p\rho_s(t) \ll 1, \\ \pi_i(t) &\approx \sum_{j=1}^{M} a_{ij}pD_j^i(t). \end{aligned} \tag{B1}$$

Substituting Eq. (B1) into Eq. (5), we can obtain the linearized equation near the disease-free equilibrium as

$$\begin{cases} \rho_i(t+1) &= (1-\mu)\rho_i(t) + \sum_{j=1}^{M}\sum_{s\neq i}^{N} a_{sj}a_{ij}p^2\lambda\rho_s(t) \\ & \quad + \sum_{j=1}^{M} a_{ij}p\lambda\gamma_j\beta_j(t-1) \\ \beta_j(t+1) &= \gamma_j\beta_j(t) + \sum_{s=1}^{N} a_{sj}p\rho_s(t+1). \end{cases} \tag{B2}$$

Define $\theta_j(t) = \gamma_j\beta_j(t-1)$, then Eq. (B2) becomes

$$\begin{cases} \rho_i(t+1) &= (1-\mu)\rho_i(t) + \sum_{j=1}^{M}\sum_{s\neq i}^{N} a_{sj}a_{ij}p^2\lambda\rho_s(t) \\ & \quad + \sum_{j=1}^{M} a_{ij}p\lambda\theta_j(t), \\ \theta_j(t+1) &= \gamma_j\theta_j(t) + \gamma_j(t)\sum_{s=1}^{N} a_{sj}p\rho_s(t). \end{cases} \tag{B3}$$

Setting $\boldsymbol{x}(t) = (\rho_1(t), \cdots, \rho_N(t), \theta_1(t), \cdots, \theta_M(t))^{\mathrm{T}}$ and $\boldsymbol{G}_0 = \mathrm{diag}(\gamma_1, \gamma_2, \cdots, \gamma_M)$, we can rewrite Eq. (B3) as

$$\boldsymbol{x}(t+1) = \boldsymbol{H}\boldsymbol{x}(t), \tag{B4}$$

where

$$\boldsymbol{H} = \begin{pmatrix} (1-\mu)\boldsymbol{I}_N + p^2\lambda\boldsymbol{K} & p\lambda\boldsymbol{A} \\ p\boldsymbol{G}_0\boldsymbol{A}^{\mathrm{T}} & \boldsymbol{G}_0 \end{pmatrix} \tag{B5}$$

and $(\boldsymbol{K})_{ss} = 0$, $(\boldsymbol{K})_{sl} = (\boldsymbol{A}\boldsymbol{A}^{\mathrm{T}})_{sl}, \forall 1 \leqslant s \neq l \leqslant N$. Obviously, $\boldsymbol{x} = 0$ is a fixed point of Eq. (B4) and is stable when $\rho(\boldsymbol{H}) < 1$. Perron-Frobenius theorem ensures that the nonnegative matrix $\boldsymbol{H}$ has a positive dominant eigenvalue. Thus, $\rho(\boldsymbol{H}) < 1$ if and only if $\lambda_{\max}(\boldsymbol{H}) < 1$. Note

$$\boldsymbol{Q} = \begin{pmatrix} \lambda^{1/2}\boldsymbol{I}_N & 0 \\ 0 & \boldsymbol{G}_0^{1/2} \end{pmatrix},$$

then $\boldsymbol{Q}^{-1}\boldsymbol{H}\boldsymbol{Q}$ is sysmmetric. Thus, all the eigenvalues of $\boldsymbol{H}$ are real and $\boldsymbol{H}$ is diagonalizable, which implies $\lambda_{\max}(\boldsymbol{H}) < 1$ if and only if $\boldsymbol{H} - \boldsymbol{I}$ is negative definite. Note

$$\boldsymbol{Q}_1 = \begin{pmatrix} \boldsymbol{I}_N & \boldsymbol{0} \\ -p(\boldsymbol{G}_0 - \boldsymbol{I}_M)^{-1}\boldsymbol{G}_0\boldsymbol{A}^{\mathrm{T}} & \boldsymbol{I}_M \end{pmatrix},$$

then

$$\boldsymbol{Q}_1^{\mathrm{T}}(\boldsymbol{H} - \boldsymbol{I})\boldsymbol{Q}_1 = \begin{pmatrix} -\mu\boldsymbol{I}_N + p^2\lambda\boldsymbol{H}_1 & p\lambda\boldsymbol{A} - p\boldsymbol{A}\boldsymbol{G}_0 \\ 0 & \boldsymbol{G}_0 - \boldsymbol{I}_M \end{pmatrix},$$

where

$$\boldsymbol{H}_1 = \boldsymbol{K} - \boldsymbol{A}(\boldsymbol{G}_0 - \boldsymbol{I}_M)^{-1}\boldsymbol{G}_0\boldsymbol{A}^{\mathrm{T}}. \tag{B6}$$

Therefore, $\boldsymbol{H} - \boldsymbol{I}$ is negative definite only if

$$\lambda_{\max}(-\mu\boldsymbol{I}_N + p^2\lambda\boldsymbol{H}_1) < 0. \tag{B7}$$

The above discussion proves that Eq. (B7) is a necessary condition for the disease-free equilibrium to be stable. In fact, our model endows $\boldsymbol{A}$ with additional properties, making the necessary condition almost surely also sufficient. Since $\boldsymbol{A}$ is a randomly generated matrix which is independent to $\boldsymbol{G}_0 - \boldsymbol{I}_M$, the probability of $\boldsymbol{H}_1$ having a common eigenvalue with $\boldsymbol{G}_0 - \boldsymbol{I}_M$ is almost 0. That means $\boldsymbol{Q}_1^{\mathrm{T}}(\boldsymbol{H} - \boldsymbol{I})\boldsymbol{Q}_1$ is almost surely diagonalizable where $\boldsymbol{Q}_1^{\mathrm{T}}(\boldsymbol{H} - \boldsymbol{I})\boldsymbol{Q}_1$ is negative definite if and only if Eq. (B7) holds. Thus, Eq. (B7) is almost surely a necessary and sufficient condition for the disease-free equilibrium to be stable.

[1] R. Pastor-Satorras, C. Castellano, P. Van Mieghem, and A. Vespignani, Rev. Mod. Phys. **87**, 925 (2015).
[2] C. Y. Liu, X. Q. Wu, R. W. Niu, M. A. Aziz-Alaoui, and J. H. Lu, IEEE Trans. Circuits Syst. I **68**, 3772 (2021).
[3] J. Liu, X. Q. Wu, J. H. Lu, and X. Wei, IEEE Trans. Syst. Man Cybern, Syst. **51**, 1085 (2021).
[4] V. Colizza, R. Pastor-Satorras, and A. Vespignani, Nat. Phys. **3**, 276 (2007).
[5] V. Colizza and A. Vespignani, J. Theor. Biol. **251**, 450 (2008).
[6] D. Balcan, V. Colizza, B. Goncalves, H. Hu, J. J. Ramasco, and A. Vespignani, Proc. Natl. Acad. Sci. USA **106**, 21484 (2009).
[7] A. Lipshtat, R. Alimi, and Y. Ben-Horin, Sci. Rep. **11**, 15198 (2021).
[8] Y. W. Gong and M. Small, Phys. Lett. A **383**, 125996 (2019).
[9] A. Apolloni, C. Poletto, J. J. Ramasco, P. Jensen, and V. Colizza, Theor. Biol. Med. Model. **11**, 3 (2014).
[10] V. Belik, T. Geisel, and D. Brockmann, Phys. Rev. X **1**, 011001 (2011).
[11] J. Gómez-Gardeñes, D. Soriano-Panos, and A. Arenas, Nat. Phys. **14**, 391 (2018).
[12] M. Rosvall, A. V. Esquivel, A. Lancichinetti, J. D. West, and R. Lambiotte, Nat. Commun. **5**, 4630 (2014).
[13] L. Feng, Q. C. Zhao, and C. Q. Zhou, Phys. Rev. E **102**, 022306 (2020).
[14] C. Granell and P. J. Mucha, Phys. Rev. E **97**, 052302 (2018).
[15] O. S. Sisodiya, O. P. Misra, and J. Dhar, Math. Biosci. **298**, 46 (2018).
[16] R. Memarbashi and S. M. Mahmoudi, Math. Methods Appl. Sci. **44**, 5873 (2021).
[17] F. Saldana, H. Flores-Arguedas, J. A. Camacho-Gutierrez, and I. Barradas, Math. Biosci. Eng. **17**, 4165 (2020).
[18] A. Matsuki and G. Tanaka, Phys. Rev. E **100**, 022302 (2019).
[19] G. Tanaka, C. Urabe, and K. Aihara, Sci. Rep. **4**, 5522 (2014).
[20] B. Wang, M. Gou, Y. K. Guo, G. Tanaka, and Y. X. Han, Phys. Rev. E **102**, 062306 (2020).
[21] S. Gomez, A. Arenas, J. Borge-Holthoefer, S. Meloni, and Y. Moreno, Europhys. Lett. **89**, 38009 (2010).
[22] G. St-Onge, H. L. Sun, A. Allard, L. Hebert-Dufresne, and G. Bianconi, Phys. Rev. Lett. **127**, 158301 (2021).
[23] R. Pastor-Satorras and A. Vespignani, Phys. Rev. E **65**, 036104 (2002).
[24] M. Kuperman and G. Abramson, Phys. Rev. Lett. **86**, 2909 (2001).
[25] R. Pastor-Satorras and A. Vespignani, Phys. Rev. Lett. **86**, 3200 (2001).
[26] C. Stegehuis, R. van der Hofstad, and J. S. H. van Leeuwaarden, Sci. Rep. **6**, 29748 (2016).